Published in final edited form as:
J Phys Chem B. 2008 December 25; 112(51): 16741–16751.

Kinetics of Bacterial Phospholipase C Activity at Micellar Interfaces: Effect of Substrate Aggregate Microstructure and a Model for the Kinetic Parameters

Jasmeet Singh[1], **Radha Ranganathan**[1,*], and **Joseph Hajdu**[2]

[1] Department of Physics and Center for Supramolecular Studies, California State University, Northridge, CA 91330-8268, U.S.A

[2] Department of Chemistry and Biochemistry and Center for Supramolecular Studies, California State University, Northridge, CA 91330-8262, U.S.A

Abstract

Activity at micellar interfaces of bacterial phospholipase C from *Bacillus cereus* on phospholipids solubilized in micelles was investigated with the goal of elucidating the role of the interface microstructure and developing further an existing kinetic model. Enzyme kinetics and physicochemical characterization of model substrate aggregates were combined; thus enabling the interpretation of kinetics in the context of the interface. Substrates were diacylphosphatidylcholine of different acyl chain lengths in the form of mixed micelles with dodecyldimethylammoniopropanesulfonate. An early kinetic model, reformulated to reflect the interfacial nature of the kinetics, was applied to the kinetic data. A better method of data treatment is proposed, use of which makes the presence of microstructure effects quite transparent. Models for enzyme-micelle binding and enzyme-lipid binding are developed and expressions incorporating the microstructural properties are derived for the enzyme-micelle dissociation constant K_S and the interface Michaelis-Menten constant, K_M. Use of these expressions in the interface kinetic model brings excellent agreement between the kinetic data and the model. Numerical values for the thermodynamic and kinetic parameters are determined. Enzyme-lipid binding is found to be an activated process with an acyl chain length dependent free energy of activation that decreases with micelle lipid molar fraction with a coefficient of about $-15\ RT$ and correlates with the tightness of molecular packing in the substrate aggregate. Thus the physical insight obtained includes a model for the kinetic parameters that shows that these parameters depend on the substrate concentration and acyl chain length of the lipid. Enzyme-micelle binding is indicated to be hydrophobic and solvent mediated with a dissociation constant of 1.2 mM.

1. Introduction

Phospholipases are interfacial enzymes that catalyze the hydrolysis of lipids aggregated in the form of mixed micelles or cell membranes. In the case of digestive enzymes, the substrates are mixed micelles of dietary lipids and bile salts [1]. Hydrolysis of phospholipids in membranes by phospholipase enzymes is the first part of the biological process of lipid metabolism [2–5]. The activity of phospholipases toward lipids in aggregated forms is significantly higher than that toward the monomeric form: hundred times or more for secretory phospholipase A_2 and two to six fold for bacterial phospholipase C [6–8]. Hydrolysis occurs at the aggregate/water interface and the mechanism of enzyme action may be specific to the phospholipase and the substrate.

*Radha.ranganathan@csun.edu.

The goal of this work is to understand in a quantifiable manner how the physicochemical nature of the interface manifests in the kinetics and level of enzyme activity. The substrates in this study are mixed micelles of phospholipids and surfactants. Micellar substrates are relevant to enzymatic reactions in the digestive tract and in other applications[9]. Properties like lipid packing leading to chain length dependence of the enzyme activity could well have the same effect in other types of substrates of relevance in membrane lipid hydrolysis. Model micellar substrates are useful for quantifying these effects and thus a platform to investigate the interfacial nature of the kinetics. Interfacial enzyme activity studies have recognized that the microstructure of the aggregate is of significance in the level of activity [10–14]. However studies of enzyme kinetics have mostly treated the aggregate as a black box. In pursuing the goals of understanding the role of aggregate microstructure and modeling the kinetics of hydrolysis at the interface, we have combined the physicochemical characterization of the substrate aggregate together with conducting enzyme kinetic studies, thus enabling the interpretation of kinetics in the context of the interface. In the work presented here, an interfacial kinetic model is further developed to account for interface microstructure effects by studying the enzymatic action of bacterial phospholipase C (*PLC*) from *Bacillus cereus* on previously characterized model substrate aggregates [15,16]. This enzyme is of interest because it is functionally and structurally similar to mammalian PLC [2,7,14,17]. A prescription is formulated to first confirm the presence of substrate aggregate microstructure effects and subsequently quantify their nature.

Enzyme kinetic characterization of *B. cereus PLC* on diacylphosphatidylcholine dispersed in micelles of the surfactant dodecyldimethylammoniopropanesulfonate (*DPS*) is performed. In recently completed work, this model substrate system was shown to have some useful properties that allow better control in investigating kinetics [16]. For example, the micelle concentration can be varied while keeping the aggregation number or the micelle composition and thereby the interface substrate concentration constant. In addition the *DPS*/lipid mixed micelles are spherical and the shape does not vary in a series of samples of varying micelle concentration. In contrast bile salt/lipid mixed micelles show variations in microstructure within such a series and complicate the interpretation of enzyme kinetics [18]. In our recent studies of *B. cereus PLC* activity on bile salt/lipid mixed micelles, a reformulated version of an early interface kinetic model was presented. When tested the model showed excellent applicability but not without concerns on the effects of microstructural variations [15]. Unlike in bulk solution kinetics, effects of the kinetic medium in interface kinetics cannot be ignored because the nature of the interface medium changes with the interface substrate concentration. The premise of the present work is then, that the original interface kinetic model continues to apply and that a kinetic characterization must include physicochemical characterization of the substrate aggregate. Having chosen a well-behaved (in the context of the microstructure) substrate system and having completed physicochemical characterization of the substrate aggregates, we continued the work on the kinetic studies. The reformulated kinetic model was applied to the kinetic data. Use of the modified form quite transparently brings forward the behavior of the kinetic parameters; thus it is found to be a better method for treating the data. From the requirements of fitting of the kinetic data to the model, insights into the nature of the variation of the activity with interface substrate concentration, the kinetic parameters and the model itself are obtained. In particular two empirical postulates, derived from present observations, that bring the data into excellent agreement with the interface kinetic model are (i) the kinetic step of formation of micelle-bound enzyme-lipid complex requires activation and (ii) the enzyme-micelle binding for bacterial *PLC* is independent of the micelle lipid composition. Expressions relating the thermodynamic and kinetic parameters to the properties of the kinetic medium are developed. The free energy barrier for the transfer of the lipid from the micelle to the enzyme is determined and found to correlate with the packing of the lipid in the micelle. The mechanism of enzyme-micelle binding is the one mediated by the solvent rather than hopping of enzyme between micelles in an intermicellar collision.

2. Materials and Methods

2.1. Model for Interface kinetics

The concerned chemical reaction involving the hydrolysis of the phosphodiester bond is described in Eq. 1.

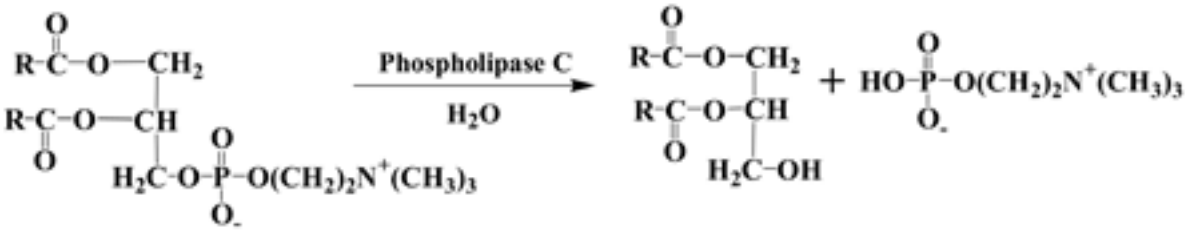

(1)

The reaction occurs at the interface in three steps [19]. The derivations of the equations for activity are available in previous work and only the essential parts are repeated here[15,19].

i. Enzyme binds to the micelle interface to form a micelle bound enzyme, E^*_{mic}

$$[E]+n\,[micelles] \underset{k_{-1}}{\overset{k_1}{\rightleftarrows}} [E^*_{mic}], \tag{2}$$

n is the number of binding sites per micelle, *[micelles]* is the concentration of micelles.

ii. The bound enzyme binds a lipid substrate in the aggregate, forming the complex $E^*_{mic}S$. *[S]* is the interface substrate concentration.

$$E^*_{mic}+[S] \underset{k_{-2}}{\overset{k_2}{\rightleftarrows}} [E^*_{mic}\,S] \tag{3}$$

iii. The enzyme catalyzes hydrolysis of the lipid in the chemical step, forming the product *P*.

$$[E^*_{mic}S] \xrightarrow{k_3} [E^*_{mic}]+[P] \tag{4}$$

Activity, defined by the rate of product formation, *v*, per mole of enzyme present, is $v/[E_T]$, where $[E_T]$ is the total enzyme concentration at the aggregate interface [19]. The steady state solution for the activity, denoted by *A* is

$$A \equiv \frac{v}{[E_T]}=\frac{k_3 n[micelles][S]}{K_S K_M+K_M n[micelles]+n[micelles][S]}, \tag{5}$$

and its inverse is

$$A^{-1}=\frac{[E_T]}{v}=\frac{K_S K_M}{k_3 n[micelles][S]}+\frac{K_M}{k_3[S]}+\frac{1}{k_3} \tag{6}$$

$$K_S=\frac{k_{-1}}{k_1};\ K_M=\frac{k_{-2}+k_3}{k_2} \tag{7}$$

The lipid surface concentration, *[S]* is the number of moles of lipid molecules per micelle per unit surface area of micelle,

$$[S]=\frac{[lipid]}{[micelles]A_{micelle}N_0}=\frac{N_{lipid}}{A_{micelle}N_0}, \tag{8}$$

where *[lipid]* is the bulk solution lipid concentration, $A_{micelle}$ is the micelle surface area, N_{lipid} is the aggregation number of the lipid molecules in the mixed micelle, and N_0 is Avogadro's number. The number of binding sites per micelle, *n*, is the ratio of micelle surface area to the area per binding site. Thus,

$$n=\frac{A_{micelle}}{a_0} \tag{9}$$

The area per binding site, a_0, may be treated as the projection of the enzyme's cross-sectional area on to the micelle surface. Use of eq. 8 and 9 in eq. 5 gives

$$A=\frac{v}{[E_T]}=\frac{k_3[S]}{C_1 k_3[S]+K_M} \tag{10}$$

where,

$$C_1=\frac{K_S K_M a_0 N_0}{k_3[lipid]}+\frac{1}{k_3} \tag{11}$$

The reciprocal of the activity is,

$$A^{-1}=\frac{[E_T]}{v}=\frac{K_S K_M a_0 N_0}{k_3[lipid]}+\frac{K_M}{k_3[S]}+\frac{1}{k_3}=C_1+\frac{K_M}{k_3}\left(\frac{1}{[S]}\right) \tag{12}$$

2.2. *Assay* and *Treatment of data*

a—The singularity of the interface nature of the kinetics *vis. à vis.* bulk solution kinetics is the dependence of the activity on *[micelles]* as well as *[S]* and the occurrence of the additional parameter K_S. Furthermore, when the medium is the interface whose properties change with

[S], the possibility that K_S and K_M are functions of *[S]* cannot be ruled out. In bulk solution kinetics, K_M is a solution property that is not expected to change with substrate concentration. Eq. 5, 6 and 10, 12 provide us with options and limits on designing assays. The two sample variables are *[micelles]* and *[S]*. Series of samples in which one variable can be varied while the other stayed constant would be desirable to begin a proper application of the kinetic model. For anionic and cationic micelles neither type of series can be realized [20–22]. In general, for nonionic and zwitterionic micelles, the micelle concentration can be varied keeping *[S]* constant but the alternative is not possible. The choice of the present zwitterionic system was motivated by this possibility and was also verified as briefly outlined below in §2.3 and in the appendix and detailed in our published work [16].

The samples for the kinetic experiments were organized into two types of series:

Constant [S] or [micelle] dilution series: In this series, the *[DPS]:[lipid]* ratio, denoted by *R*, was constant while the total concentration C_T = *[DPS]+[lipid]* was varied. This series is a constant composition series. As per the characterization experiments, in a constant composition series the micelle concentration varies with C_T while the micelle aggregation and composition remain constant [16]. Thus in a constant composition series the micellar lipid concentration and the interface properties are constant and this series is a constant *[S]* series as well.

Constant [lipid] or surface dilution series: In this series the solution lipid concentration was constant and the *DPS* concentration was varied. As *[DPS]* increases, the micelle concentration increases and the micellar lipid composition, X_{lipid}^{mic}, decreases. This series thus represents a surface dilution series. Across this series, the properties of the reaction medium, namely the interface, do change.

b—For a micelle dilution series, in which *[S]* is constant, one may choose to use eq. 6 and view the activity data as a function of *[micelles]*. However a better choice is to use eq. 12 and treat the activity as a function of *[lipid]*. If the kinetic parameters were dependent only on *[S]* apart from other absolute constants, then A^{-1} varies linearly with $[lipid]^{-1}$ with slope and intercept:

$$\text{Slope of } A^{-1} \text{ vs.} [\,lipid]^{-1} \equiv \zeta = \frac{K_s K_M a_0 N_0}{k_3}, \tag{13}$$

$$\text{Intercept of } A^{-1} \text{ vs.} [\,lipid]^{-1} \equiv J = \frac{K_M}{k_3 [S]} + \frac{1}{k_3}. \tag{14}$$

Furthermore, if the kinetic parameters were constant, ζ would not vary from one micelle dilution series of a certain *[S]* to another of a different *[S]* and *J* would vary inversely with *[S]*. Any systematic deviation from such behavior is clue to the presence of aggregate microstructure effects. A deviation is indeed observed and its dependence on *[S]* is analyzed to develop hypotheses for the physicochemical nature of the enzyme-micelle and enzyme-lipid binding, the effects of substrate aggregate microstructure and the structure of K_S and K_M. The hypotheses based model expressions for these parameters are then incorporated into the kinetic model. Application of the resulting expanded model, in addition to reassuringly describing the data, yields numerical values for the various constants in those model expressions. Use of these constants and the model to calculate the activities for the surface dilution series reproduces the experimental data on those series remarkably well.

2.3 Chemicals and Experimental Methods

a—The lipids, 1,2-Dilauroyl-*sn*-glycero-3-phosphocholine (*DLPC*), 1,2-Dimyristoyl-*sn*-glycero-3-phosphocholine (*DMPC*), and 1,2-Dipalmitoyl-*sn*-glycero-3-phosphocholine (*DPPC*), were obtained from Avanti Polar Lipids as lyophilized powders. The surfactant, 3-Dodecyldimethylammoniopropanesulfonate (*DPS*, >98%) was obtained from Sigma and was used without further purification. Pyrene (optical grade, 99%, Aldrich) and 3,4-dimethyl benzophenone (*DMBP*, 99%, Aldrich) were used as fluorescence probe and quencher respectively for physicochemical characterization of the substrate by time resolved fluorescence quenching (*TRFQ*). 5-doxyl stearic acid methyl ester (5DSE; 99% Sigma), was used as spin probe in the *ESR* experiments. Phospholipase C (*PLC*) from *Bacillus cereus* was obtained from Sigma as a lyophilized powder. It was purified by dialysis against 0.05M sodium phosphate buffer at pH 8.0 for three days, changing the buffer every 8 hours. Protein concentration was determined by the method of Lowry et al.[23] using bovine serum albumin (*BSA*) as standard and also by the extinction coefficient method [24,25]. Lowry's method involves the complexation between protein molecules and copper ions of Lowry's reagent, which changes the color of the protein solution to blue. It requires a precise timing of readings because color instability can produce considerable error in the measurement [25]. On the other hand, the extinction coefficient method does not involve any external reagent; therefore errors are much smaller in this method. Both of these methods gave results consistent to within ±5%. The purified enzyme was stored at pH 8.0 in 0.05M sodium phosphate buffer at 4°C.

b. Mixed micelle solution preparation—The solution compositions and concentrations in the constant *[lipid]* series were (i) *[lipid]* = 4mM and *[DPS]* ranging from 8 to 80mM (ii) *[lipid]* = 10mM and *[DPS]* ranging from 20 to 200mM. For each sample solution, the appropriate amount of *DMPC* powder was mixed with few drops of ethanol. The resulting ethanol solution mixture was vortexed thoroughly to produce a clear solution which was then dried under dry N_2 flux to produce a film of *DMPC*. Thereafter, the required amounts of the *DPS* surfactant and water were added to the dry film to achieve the final concentrations. The solution was stirred overnight to ensure the complete solubilization of phospholipid in surfactant micellar solution. For the constant *[S]* series, stock solutions with *[lipid]* =20mM and *[DPS]* ranging from 40 to 200mM, were prepared as described above. These stock solutions were diluted subsequently with appropriate amounts of water to get different sample solutions with constant *[DPS]/[lipid]* ratio but different total concentration. The composition of the solution is expressed in molar fraction (X_{DMPC}) of *DMPC*, or molar ratio (R) of *DPS* to lipid and the micelle composition is the molar fraction of lipid in the micelle written as X_{lipid}^{mic} defined by,

$$X_{lipid}=\frac{[lipid]}{C_T};\ R=\frac{[DPS]}{[lipid]};\ X_{lipid}^{mic}=\frac{[lipid]}{C_T-[M_{free}]} \tag{15}$$

The aqueous concentration of the unassociated monomers, M_{free} is negligible compared to the total concentration, C_T; therefore X_{lipid}^{mic} can justifiably be approximated by X_{lipid} 16.

c. Enzyme activity—The activity of enzyme is the amount of phosphorylcholine released per milligram of enzyme per unit time. It is measured in units of μmol of acid released, due to lipid hydrolysis, per minute per milligram of enzyme (μmol/min/mg). The enzyme activity measurements were conducted employing standard pH-stat methods [1]. The activity of *PLC* in mixed micelles of *DPS/lipid* was measured by addition of 20 μL of enzyme (0.084 μg) into 5 mL of mixed micelles solutions, and monitoring the amount of 0.01 M *NaOH* required per minute to maintain a constant pH of 8.00 using a Radiometer pH-stat assembly consisting of

a titrator, an auto burette, and a pH meter, Model TIM 854 electrode, interfaced to a computer for recording data. The principle behind this method is the deprotonation of the phosphorylcholine released by the chemical reaction that causes the pH to drop and the amount of *NaOH* needed to bring the pH back to a preset value is a measure of enzyme activity. The reaction was followed for 8 min. The initial rate of activity was determined from the first 2 to 4 min of data. The yield increases linearly with time and the slope of the line divided by the mass of the enzyme in mg gives the activity, in units of μmol/min/mg. The error in the fitted slopes was < 1%. All activity measurements were conducted at 40 °C. Before any hydrolysis measurement, the stability of the enzyme was checked by measuring its activity towards a standard assay system. Two different standard assay mixtures used to determine the activity of *PLC* were (i) egg yolk emulsion and (ii) one of the *DPS+DMPC* mixtures of a selected concentration/composition. The egg yolk assay was used to determine the activity of the enzyme following the method described by Nieuwenhuizen et al. [26]. The observed activity of freshly dialyzed *PLC* was 1400 (±4%) μmol/min/mg. The stock solution of *PLC* showed no loss of enzymatic activity for over a period of several weeks. The composition of the *DPS +DMPC* mixture selected as a control was *[DMPC]* = 4mM and *[DPS]* = 8mM. This system was preferred over the egg yolk assay because the lecithin content and composition may vary in different egg yolks. The observed activity in *DPS+DMPC* assay mixture was 2400 (±4%) μmol/min/mg. This reference system was measured before, at the middle and at the end of every series of experiments to reassure the reproducibility of results. The precision error in the activity determined from about fifty repeated measurements on the control sample, with the same batch of enzyme under the same experimental conditions, over the course of the entire set of experiments, was ±4%. The activity value was found to differ by a maximum of about 15 % between different batches of enzyme or the same enzyme solution kept over two months and different instrument warm-up times. For example, available methods to determine enzyme concentration can only estimate the concentration to within 10%. So working with the same batch was found to improve precision and thus more meaningful. Therefore care was taken to maintain identical experimental conditions and the experiments were conducted in the shortest time possible. These cautionary measures are believed to have led to the minimal scatter in the data so that reliable conclusions could be drawn.

d. Physicochemical characterization of substrate aggregates—Micelle aggregation numbers, N_{lipid} and N_{DPS}, are obtained from time-resolved fluorescence quenching *(TRFQ)* and the micelle hydration indexed by the volume fraction of water in the polar micelle/water interface, from electron spin resonance *(ESR).* The measurements were conducted at sample temperatures of 40°C. The TRFQ and ESR data are combined together in a molecular space filling model which treats the mixed micelle as an entity of the two types of monomers and water. The calculations yield the geometrical features of the micelle. Use of the aggregation numbers and the calculated micelle area in eq. 8 gives *[S]*. Results of the previous characterization experiments on *DPS*/dimyristoylphosphatidylcholine (*DMPC*) and several additional measurements as required on the other lipid mixed micelles are used here. The techniques are described in previous publications [15,16]. Additional information and data are provided in the appendix.

3. Results and Model for K_S and K_M

The curves in Fig. 1 are representative of the reaction progress curves. Numerical values for the activity (eq. 5 and §2.3c) are obtained from the slopes of reaction progress curves and treated according to the protocol described in §2.2b. For the six *[micelle]* dilution series each of constant composition or *[S]*, the reciprocals of the activity are viewed against the reciprocals of *[lipid]* as in Fig. 2. The data indicate linear variation and do not exhibit scatter, presumably due to the precautions exercised as described in Section 2c. The slopes, ζ, of the linear variation according to eq. 13, being solely dependent on constants and on K_S, K_M, and k_3, would be

constant if these parameters were constant. The slopes however, as found in Fig. 3, decrease with increase in *[S]* or X_{lipid}^{mic}. The heterogeneity in slopes was tested using a general linear model with an interaction term between *[S]* treated as categorical and $[lipid]^{-1}$. The slopes were significantly heterogeneous for all three lipids (DLPC: $F_{5,45}$=10.199, P<0.001, R^2=0.998; DMPC: $F_{5,45}$=76.283, P<0.001, R^2=0.999; DPPC: $F_{5,48}$=142.200, P<0.001, R^2=0.999) The test was implemented in SYSTAT 200. For each lipid, the low P-value justifies rejection of the null hypothesis that the slopes are homogeneous, given the data. The R^2 values indicate that almost all the variation in inverse enzyme activity was explained by fitting lines with separate slopes.

Note that X_{lipid}^{mic}, aggregation numbers and thereby the micelle area, A_{mic} remain constant in the constant *[S]* series. This means, *[S]* and X_{lipid}^{mic} are linearly proportional to each other in this series and any functional variation with *[S]* can be regarded as a variation with X_{lipid}^{mic} as well. A preliminary examination of Fig. 3 suggested an exponential dependence. This gives good reason to hypothesize that the kinetic parameters are not constants because they can depend on the micellar microstructure which changes with *[S]*. The standpoint here is that the interface kinetic model is basically sound because it is based on reasonable hypotheses as represented by the kinetic steps (eq. 2–4) and that the possibility of the microstructural dependence of kinetic parameters needs to be examined. The exponential nature of the dependence suggests that some of the kinetics might be of the nature of Arhenius type of activated processes because rate constants of such processes depend exponentially on a free energy of activation and that this activation free energy depends on X_{lipid}^{mic}. Furthermore, the slope does not tend to zero for large X_{lipid}^{mic}. Possible effects the microstructure can have on the rate constants of the various kinetic steps and thereby on the parameters, K_S and K_M, are now considered.

3.1. Effect of microstructure on K_M

Following the conventional theories for rate constants, the model proposed for the rate constant k_2 and k_{-2}, that was also found to explain the data, is as follows. In the kinetic step (ii) the lipid binds to the micelle-bound enzyme. This step is visualized in Fig. 4a. The enzyme bound lipid and the micelle solubilized lipid are two thermodynamic states with a free energy barrier in between, Fig. 4b. In both of these states the lipid is in the micelle, as depicted in Fig. 4a, that visualizes the lipid as reaching out of the micelle, binding to the enzyme and anchoring the enzyme to the micelle [19,27–29]. In the process the lipid transfers across a free energy barrier from one micro environment to another. The higher the barrier the slower the rate of transfer, so that k_2 and k_{-2} as might be expressed for activated processes are;

$$k_2 \alpha exp\left(-\frac{|\Delta g_{left}|}{RT}\right)$$
$$k_{-2} \alpha exp\left(-\frac{|\Delta g_{right}|}{RT}\right) \quad (16)$$

The height of the barrier, $|\Delta g_{left,\ right}|$, is the magnitude of the molar free energy difference between the free energy of the lipid at the top of the barrier (“transition state”) and the lipid in the micelle (left side in Fig. 4b) or lipid –enzyme-micelle complex (right side in Fig. 4b); R is the gas constant. Taking the free energy per lipid molecule to be 0 at the top, the heights of the barrier for the forward and reverse transfers are written down first and subsequently explained:

$$|\Delta g_{left}| = g_{0m} - g_1 X_{lipid}^{mic} + RT(X_{lipid}^{mic}\, ln\, X_{lipid}^{mic} + (1 - X_{lipid}^{mic}) ln(1 - X_{lipid}^{mic}))$$
$$|\Delta g_{right}| = g_{0e} - g_1 X_{lipid}^{mic}. \quad (17)$$

The free energy of the lipid in the micelle, $|\Delta g_{left}|$, increases from some initial value $-g_{0m}$ with contributions from the internal energy of molecular interactions, the entropy (configuration), and the entropy of mixing, ΔS_{mix} $(= -R(X_{lipid}^{mic}\, ln\, X_{lipid}^{mic} + (1 - X_{lipid}^{mic}) ln(1 - X_{lipid}^{mic}))$. In a first approximation, we write the internal energy and the configuration entropy part to be linear in X_{lipid}^{mic} with a coefficient g_1. The enzyme-bound lipid is bound to the micelle as well and its free energy, $|\Delta g_{right}|$ increases also as X_{lipid}^{mic} from some base value $-g_{0e}$, but without the entropy of mixing.

Rewriting eq. 16 for k_2 and k_{-2} using eq. 17 gives,

$$k_2\, \alpha\, exp\left(-\frac{|\Delta g_{left}|}{RT}\right) = k_{20}\, exp\left(\frac{g_1 X_{lipid}^{mic}}{RT} - (X_{lipid}^{mic}\, ln\, X_{lipid}^{mic} + (1 - X_{lipid}^{mic}) ln(1 - X_{lipid}^{mic})\right)$$
$$k_{-2}\, \alpha\, exp\left(-\frac{|\Delta g_{right}|}{RT}\right) = k_{-20}\, exp\left(\frac{g_1 X_{lipid}^{mic}}{RT}\right) \quad (18)$$

The pre-exponent terms k_{20} and k_{-20} now include the g_{0m} and g_{0e} terms respectively. Eq. 18 expresses the relation that the free energy per lipid molecule in the mixed micelle increases with the increase in the molar fraction of the lipid. The idea expressed by eq. 18 is that as lipid content in the micelle is increased, the transfer of the lipid between the micelle and the enzyme becomes easier, because the height of the barrier becomes shorter. To understand this physically, the micelle may be viewed as an assembly of molecules that become increasingly tightly packed as more lipids are introduced. The tightness of packing is reflected by the increase in microviscosity (or decrease in fluidity) and decreased hydration index (see data in appendix)[16]. The increased tightness of packing causes the micelle lipid free energy to increase and the barrier for transfer consequently reduces. The rate constant k_3 is independent of the micelle lipid composition because the catalytic step occurs after the capture of the lipid by the enzyme and the micelle involvement does not change in this process. The parameter K_M may then be written as,

$$K_M = \left[K_{M00} + K_{M0}\, exp\left(-\frac{g_1 X_{lipid}^{mic}}{RT}\right)\right] exp\left(X_{lipid}^{mic} ln X_{lipid}^{mic} + (1 - X_{lipid}^{mic}) ln(1 - X_{lipid}^{mic})\right)$$
$$K_{M00} = \frac{k_{-20}}{k_{20}},\quad K_{M0} = \frac{k_3}{k_{20}}. \quad (19)$$

3.2. Effect of microstructure on K_S

The parameter K_S of step (i) is the enzyme-micelle dissociation constant, and is determined by the ratio of the micelle dissociation rate to the micelle association (or binding) rate constant. The bacterial *PLC* enzyme was found to bind to the *DPS* micelle even in the absence of lipid. Evidence was obtained from measurements of micelle hydration by *ESR* methods (Fig. A3). The hydration index of *DPS* micelles was measured with and without the presence of *PLC* in solution. The hydration index of *DPS* micelle decreased from 44 % in the absence of enzyme to 40 % percent in the presence of 0.4 mg/ml of enzyme. This indicates that the enzyme binds to the micelle irrespective of the presence of the lipid and displaces water from the micelle

headgroup area, which is observed as a decrease in hydration. This finding is supported by studies using gel filtration chromatography that demonstrated binding of *PLC* to ionic, zwitterionic, and non-ionic detergent micelles not containing lipids [30]. In view of this we treat K_S of the initial binding step for micelle and *PLC* to be independent of X_{lipid}^{mic}. Another phenomenon that can influence the enzyme-micelle dissociation rate constant is the hopping of the bound enzyme from one micelle to another during a collision between micelles [31]. Hopping includes this form of direct jump in addition to enzyme dissociation/association with the micelle through the solvent. The rate of hopping involving transfer in a collision, k_h,, is then given by the collision rate of micelles which is proportional to the micelle concentration. The transfer jump is taken to be instantaneous, so that the micelle association rate is not affected, but the dissociation rate constant is increased by k_h, so that K_S becomes,

$$K_s=\frac{k_-+k_h}{k_+}=\frac{k_-+k_{ho}[micelle]}{k_+}=K_{s0}+\alpha[micelle]=K_{s0}+\alpha\frac{(1+R)[lipid]}{N_T}, \tag{20}$$

where K_{S0} replaces $\frac{k_-}{k_+}$, the enzyme-micelle dissociation constant in the absence of hopping; k_{h0} is the proportionality between k_h and *[micelle]* and α replaces $\frac{k_{h0}}{k_+}$. In the last equality, the micelle concentration is expressed as $\frac{[DPS]+[lipid]-[M_{free}]}{N_T}\approx\frac{[DPS]+[lipid]}{N_T}=\frac{(1+R)[lipid]}{N_T}$, where N_T is the total aggregation number and R is the ratio of *[DPS]:[lipid]*.

The scooting mode of enzyme-lipid association in which the enzyme is tightly bound to a micelle and stays on that micelle is unlikely for the present substrate system. The observation of sustained activity over more than 5 minutes and the level of activity observed precludes the possibility that the enzyme remains on the same micelle because the number of lipids per micelle is typically about 15 to 20 and they would be hydrolyzed in a short time and secondly the only micelles that participate would be those with the enzyme on them leading to low levels of activity.

3.3. Effect of microstructure on Activity

Introducing the above structures of K_S and K_M into eq. 12 yields

$$A^{-1}=\frac{[E_T]}{v}=\frac{K_{S0}\left[K_{M00}+K_{M0}exp\left(-\frac{g_1X_{lipid}^{mic}}{RT}\right)\right]exp\left(X_{lipid}^{mic}lnX_{lipid}^{mic}+(1-X_{lipid}^{mic})ln(1-X_{lipid}^{mic})\right)a_0N_0}{k_3[lipid]}+\left(\frac{\left[K_{M00}+K_{M0}exp\left(-\frac{g_1X_{lipid}^{mic}}{RT}\right)\right]exp\left(X_{lipid}^{mic}lnX_{lipid}^{mic}+(1-X_{lipid}^{mic})ln(1-X_{lipid}^{mic})\right)}{k_3[S]}\right)\left((1+\alpha\frac{(1+R)a_0N_0[S]}{N_T}\right)+\frac{1}{k_3}. \tag{21}$$

The slope of the inverse activity vs. inverse [lipid], (eq. 13) no longer constant, varies with the lipid composition of the micelle as,

$$Y_S \equiv \frac{\zeta}{exp\left(X^{mic}_{lipid}\, ln\, X^{mic}_{lipid} + (1-X^{mic}_{lipid}) ln(1-X^{mic}_{lipid})\right)} = \frac{K_{S0} K_{M0} a_0 N_0}{k_3}\left[\frac{K_{M00}}{K_{M0}} + exp\left(-\frac{g_1 X^{mic}_{lipid}}{RT}\right)\right] \quad (22)$$

where the slope is modified to Y_S as defined above for convenience of graphing and clarity of presentation. The prediction of eq. 22 is that Y_S varies exponentially with X^{mic}_{lipid}. The experimental values of Y_S are examined for this behavior in Fig. 5. A fit yields g_1, $\frac{K_{M00}}{K_{M0}}$ and $\frac{K_{S0} K_{M0} a_0 N_0}{k_3}$. The intercept, *J*, of Fig. 5 can also be examined. The model in eq. 21 predicts the composition dependence of the intercept, *J*, to be,

$$J = \frac{K_{M0}}{k_3[S]}\left[\frac{K_{M00}}{K_{M0}} + exp\left(-\frac{g_1 X^{mic}_{lipid}}{RT}\right)\right] exp\left(X^{mic}_{lipid}\, ln\, X^{mic}_{lipid} + (1 - X^{mic}_{lipid}) ln(1 - X^{mic}_{lipid})\right) \left(1 + \alpha \frac{(1+R) a_0 N_0 [S]}{N_T}\right) + \frac{1}{k_3} \equiv \frac{K_{M0}}{k_3} F_i([S]) + \frac{1}{k_3}, \quad (23)$$

where $F_i([S])$ denotes the micelle composition dependent part of *J*. The function $F_i([S])$ is first calculated from the known values of *[S]*, the compositions; *R* and X^{mic}_{lipid}, the aggregation number N_T and the fit results of Y_S vs. X^{mic}_{lipid} (Fig. 5) for g_1 and K_{M00}/K_{M0} and $\alpha = 0$. α is then adjusted to find that value which gives the best straight line for *J* vs. $F_i([S])$. The resulting plots of such a procedure are shown in Fig. 5b. The best fit to a straight line was obtained for $\alpha = 0$. This means that hopping is insignificant and that the solvent mediated enzyme-micelle binding is the dominant mechanism. The slope and intercept of *J* vs. $F_i([S])$, then give the constants $\frac{K_{M0}}{k_3}$ and $\frac{1}{k_3}$. In summary, between Y_S vs. X^{mic}_{lipid} and *J* vs. $F_i([S])$, we have g_1, $\frac{K_{M00}}{K_{M0}}$ and $\frac{K_{S0} K_{M0} a_0 N_0}{k_3}$ and $\frac{K_{M0}}{k_3}$ and $\frac{1}{k_3}$, from which the parameters K_{M00}, K_{M0}, K_{S0}, *and* k_3 can be individually calculated using a model value for a_0 (425 Å^2) 19. The parameters thus derived are presented in Table 1.

In Fig. 6, we cross-check how the model works for the surface dilution series in which neither the micelle concentration nor *[S]* is constant. Using the derived values of the kinetic constants given in Table 1, the activities are calculated for several values of *[S]*. The measured and calculated activities are found to be in excellent agreement.

4. Discussion

The main significance of the work presented is in providing an improved kinetic scheme toward mechanistic elucidation of enzymatic lipolysis. Specifically, the interface medium effects were expressed by the substrate concentration dependence of the kinetic parameters. From the observation that the experimentally determined slopes, $\zeta \equiv \frac{K_S K_M a_0 N_0}{k_3}$, of A^{-1} *vs.* $[lipid]^{-1}$ of different series each of a different *[S]*, varied exponentially with X^{mic}_{lipid} (Fig. 3), the model for K_M was developed with the ratiocination that an exponential variation of kinetic rate constants could have their origin in Arhenius type activated processes. The activation barrier for lipid transfer to and from the enzyme bound state was approximated to decrease linearly with the

lipid composition of the micelle and consequently the rate constants of transfer, k_2 and k_{-2}, would increase with packing of more lipids in the micelle. This was favored by the physical reasoning that as the lipid component increases, the micelle becomes more packed and facilitates the release of the lipid. There is no direct quantifying parameter for tightness of packing. Rather it is a term signifying lack of ease of motion for a component molecule due to crowding. If the microviscosity were to be taken as an indicator of the tightness of packing, then the physicochemical characterization experiments do show that this property increases with X_{lipid}^{mic} (Fig. A2). However, the correlations described by increase in packing leading to decrease in barrier height leading to increase in k_2 cannot be carried on indefinitely, because if the molecular motion reaches a rigid limit or, in the extreme case, freezes then it means k_{20} itself is not viable. Otherwise vesicles (with tighter packing) would be more efficient than micelles as substrates, but this is not so[32]. Reduced activity in vesicles, membranes, and monolayers at increased surface pressures has been attributed to tightness of packing because a portion of the enzyme needs to insert itself into the lipid structure prior to hydrolysis [10,33,34]. Activity measurements were carried out on *DPPC* vesicles, which were prepared by vortexing a solution of 4 mM *DPPC* in water for ten minutes. The activity was found to be 75 μmol/min/mg, considerably lower than that in *DPPC/DPS* micelles (Fig. 2c and 6c). Comparison of the derived values of g_1 (Table 1) for the different lipids shows that $g_{1DLPC} < g_{1DMPC} < g_{1DPPC}$: as the acyl chain length increases the free energy coefficient for composition dependence increases. When interpreted in terms of packing, the longer the fatty acid chain length the tighter the packing. The *DPS/DPPC* mixed micelles exhibit the greatest increase in microviscosity from the value at $X_{lipid} = 0$, followed by *DPS/DMPC* and then *DPS/DLPC* corroborating that longer chain lipids experience tighter packing (Fig. A2). This does not mean that the barrier height for enzyme binding decreases and k_2 increases with chain length because the zero of the free energy need not be the same for the different lipids. So g_1 values cannot be used to compare k_2 of the different lipids. Chain length dependence of the activity was observed in some early work[35]. The present data suggest that these differences might be related to the differences in the kinetic constants due to the packing structure. Packing, lipid configuration, and strength of enzyme-lipid binding may also affect the catalytic rate, k_3, which is observed to decrease with chain length. The chemical step occurs when the lipid is enzyme-bound. In this state, the longer chain lipid being more hydrophobic may be less strongly enzyme-bound than a shorter chain lipid, (that is, longer the lipid chain lesser the free energy advantage in being enzyme-bound or smaller the $|g_{0m}-g_{0e}|$; Fig. 4b) making its proximity to the enzyme less probable and resulting in smaller k_3.

The bacterial phospholipase C enzymes are water-soluble and also bind to the interface. The possibility of enzyme hopping between collision partners during an intermicellar collision was included by writing K_S as a sum of the solvent mediated dissociation constant, K_{S0} and a part due to hopping written as $\alpha[micelles]$ to account for the micelle concentration dependence of the micelle collision rate (eq. 20). The present observations are that the bacterial *PLC* binds strongly to *DPS/lipid* mixed micelles with a dissociation constant for solvent mediated binding, $K_{s0}(=\frac{k_{-1}}{k_1}) \approx 1.2\ \mathrm{mM}$. The enzyme binds to the *DPS* micelle even in the absence of lipids (Fig. A3). A value of zero for the hopping coefficient α implies that the probability of enzyme hopping between micelles is slim. Strong hydrophobic binding is indicated because such a binding would prevent the enzyme from disengaging easily from the original micelle and transferring to the second micelle in an intermicellar collision. The nature of interface binding has not been clearly established. It could be both of non-specific binding via hydrophobic peptide parts and binding of a specific residue to the zwitterionic detergent [7,10,28,36].

5. Summary and Conclusions

We adopted and developed the model of Deems et al. and found that the improved scheme facilitates derivation of microstructural effects from the kinetic data [19,30]. Rewriting the original kinetic equations in terms of micellar properties recognizes the activity as an interface phenomenon. Substrate aggregates with proven physicochemical properties permitted design of reliable assays and controlled investigation. The method of viewing and treating the data as in Fig. 2–5, was found to be an eminent approach to investigating aggregate microstructure effects.

The main contributions of this work are the new physical insights into the kinetic model with respect to how the substrate aggregate microstructure is placed *vis. à vis.* the parameters of the model and the expressions for the thermodynamic and kinetic parameters. The greater structure brought to the original kinetic model was able to describe experimental data on the activity of bacterial phospholipase C on phosphatidylcholine substrates very well. The main findings of this investigation are that the enzyme-lipid binding that occurs at the interface is an activated process with a free energy of activation that depends on the packing structure of the lipid in the micelle because of which the level of activity depends on the lipid chain length; enzyme hopping between micelles is not significant compared to the solvent mediated enzyme-micelle binding. The constants derived from fitting of the data are physically reasonable. Experiments with other phospholipid metabolizing enzymes such as phospholipase A_2 and phospholipase D may provide answers on the scope and limitations of the model in describing kinetic profiles of interfacial catalysis. The present experimental data nevertheless support the hypothesis on the role of the interface in the reaction. The newly developed parameter structures in this work quantify that role.

Acknowledgments

This project was supported by the NIH through the grant S06 GM048680. The authors thank Professor Paul Wilson of the Department of Biology for performing the statistical tests on the data.

References

1. Hoffman WJ, Vahey M, Hajdu J. Archives of Biochemistry and Biophysics 1983;221(2):361. [PubMed: 6838196]
2. Martin SF, Follows BC, Hergenrother PJ, Franklin CL. J Org Chem 2000;65:4509. [PubMed: 10959851]
3. Dennis EA. The J Biol Chem 1994;269:13057.
4. Dennis EA. Trends Biochem Sci 1997;22:1. [PubMed: 9020581]
5. Dennis EA. Am J Respir Crit Care Med 2000;161:S32. [PubMed: 10673223]
6. Berg OG, Gelb MH, Tsai MD, Jain MK. Chem Rev 2001;101(9):2613. [PubMed: 11749391]
7. Tan CA, Roberts MF. Biochemistry 1998;37(12):4275. [PubMed: 9521750]
8. Lewis K, Garigapati VR, Zhou C, Roberts MF. Biochemistry 1993;32:8836. [PubMed: 8395883]
9. Biasutti MA, Abuin EB, Silber JJ, Correa NM, Lissi EA. Advances in Colloid Science 2008;136:1.
10. Drin G, Scarlata S. Cell Signal 2007;19:1383. [PubMed: 17524618]
11. Tatulian SA, Biltonen RL, Tamm LK. Journal of Molecular Biology 1997;268(5):809. [PubMed: 9180373]
12. Tatulian SA. Biophys J 2001;80:789. [PubMed: 11159446]
13. Ray S, Scott JL, Tatulian SA. Biochemistry 2007;46(45):13089. [PubMed: 17944488]
14. Ahyayauch H, Villar AVAA, Goni FM. Biochemistry 2005;44(34):11592. [PubMed: 16114896]
15. Ranganathan R, Tcacenco CM, Rosseto R, Hajdu J. Biophys Chem 2006;122:79. [PubMed: 16556477]
16. Singh JS, Miller J, Ranganathan R. J Phys Chem B 2007;111(31):9317. [PubMed: 17629323]

17. Titball RW. Microbiological Reviews 1993;52:347. [PubMed: 8336671]
18. Singh J, Unlu Z, Ranganathan R, Griffiths PC. J Phys Chem B 2008;112(13):3997. [PubMed: 18335917]
19. Deems RA, Eaton BR, Dennis EA. J Biol Chem 1975;250(23):9013. [PubMed: 1194274]
20. Quina FH, Nassar PM, Bonilha JBS, Bales BL. J Phys Chem 1995;99:17028.
21. Ranganathan R, Okano LT, Yihwa C, Quina FH. Journal of Colloid and Interface Science 1999;214:238. [PubMed: 10339364]
22. Abdel-Rahem R. Adv in Colloid Interface Sci 2008;114:24. [PubMed: 18378208]
23. Lowry OH, Rosebrough NJ, Lewis Farr A, Randall RJ. J Biol Chem 1951;193:265. [PubMed: 14907713]
24. Scopes RK. Analytical Biochemistry 1974;59:277. [PubMed: 4407487]
25. Stoscheck CM. Methods in Enzymology 1990;182:50. [PubMed: 2314256]
26. Nieuwenhuizen W, Kunze H, De Haas GH. Methods Enzymol 1974;32B:147. [PubMed: 4475346]
27. Zhou C, Qian X, Roberts MF. Biochemistry 1997;36:10089. [PubMed: 9254604]
28. Seetharam B, Tiruppathi C, Alpers D. Archives of Biochemistry and Biophysics 1987;253:189. [PubMed: 3813562]
29. Soltys CE, Bian J, Roberts MF. Biochemistry 1993;32:9545. [PubMed: 8373761]
30. Burns RA, El-Sayed MH, Roberts MF. Proc Natl Acad Sci Biochemistry 1982;79:4902.
31. Jain MK, Berg O. Biochim et Biophys Acta 1989;1002:127.
32. Goldfine H, Johnston N, Knob C. J Bacteriology 1993;175:4298.
33. Boguslavsky V, Rebecchi M, Morris AJ, Jhon DY, Rhee SG, McLaughlin S. Biochemistry 1994;33:3032. [PubMed: 8130216]
34. James SR, Paterson A, Harden TK, Demel RA, Downes CP. Biochemistry 1997;36:848. [PubMed: 9020783]
35. Roberts MF, Otnaess AB, Kensil CA, Dennis EA. The Journal Of Biological Chemistry 1978;253:1252. [PubMed: 624729]
36. Flesch FM, Yu JW, Lemmon MA, Burger KNJ. Biochem J 2005;389:435. [PubMed: 15755258]
37. Ranganathan R, Tran L, Bales BL. J Phy Chem B 2000;104:2260.
38. Bales BL, Ranganathan R, Griffiths PC. J Phys Chem B 2001;105(31):7465.
39. Ranganathan R, Giongo C, Bakshi MS, Bales BL, Hajdu J. Chem Phys Lipids 2005;135:93. [PubMed: 15854628]
40. Gehlen MH, De Schryver FC. Chem Rev 1993;93(1):199.
41. Almgren M, Löfroth JE. Journal of Colloid and Interface Science 1981;81:486.
42. Almgren, M. Kinetics of Excited State Processes in Micellar Media. In: Grätzel, M.; Kalyanasundaram, K., editors. Kinetics and Catalysis in Microheterogeneous Systems. Marcel Dekker, Inc.; New York: 1991. p. 63
43. Tachiya M. Chem Phys Lett 1975;33:289.
44. Bales BL, Messina L, Vidal A, Peric M, Nascimento OR. J Phys Chem 1998;102:10347.
45. Ranganathan R, Peric M, Medina R, Garcia U, Bales BL, Almgren M. Langmuir 2001;17:6765.
46. Bales BL, Zana R. J Phys Chem B 2002;106(8):1926.

Appendix

a. Physicochemical Characterization data

The methods used to obtain the microstructural data used in this work are amply described in our previous publications [16, 37–39]. Only a brief outline and data are presented here.

In *TRFQ* methods, the quenched fluorescence decay of hydrophobic fluorophores solubilized in micelles is measured [40–42]. Employing Pyrene as the fluorescence probe and dimethylbenzophenone (*DMBP*) as the quencher, *TRFQ* measurements were carried out on several *DPS*/lipid micellar solutions of various compositions. The micelle concentrations and

the aggregation numbers were determined from fits of the decay curves to the Infelta-Tachiya micellar quenching model [43]. The composition dependence of the aggregation numbers is given in Fig. A1.

Electron Spin Resonance (*ESR*) methods employ spin probes incorporated into the micelle to determine the micelle hydration index, *H*, defined by the polarity or the volume fraction of water in the environment of the spin probe and the microviscosity, η_{micro}, of the micelle/water interface[16,44]. Using 5-doxyl stearic acid methyl ester (*5DSE*), *H* and η_{micro} were determined for the same micellar solutions that were characterized by *TRFQ*. The composition dependences of *H* and η_{micro} are shown in Fig. A2. The precision errors in *H* and η_{micro} are < 1%.

The geometrical properties of the micelle; including micelle radius, interface thickness and volume, micelle surface area were then determined by model calculations using the experimentally determined aggregation numbers and hydration indices [16,38,45].

b. Enzyme-micelle binding

Any extraneous molecule when solubilized in a micelle or bound to a micelle displaces water from the interface[16,38,46]. This is seen as a reduction in the measured *H* in a spin-probe *ESR* experiment. Thus spin probes can be candidates for measuring binding. In this work we were interested only in the basic report on whether the enzyme bound to the micelle or not. On the premise that the enzyme binding to a micelle causes a reduction in *H*, we measured *H* using ESR of *5DSE* for *DPS* micellar solutions without and with enzyme at various concentrations. The results are shown in Fig. A3. Significant reduction in *H* is observed and is taken as signifying the presence of strong binding to the *DPS* micelle. The reduction for *[DPS]* = 50 mM is greater than when *[DPS]* = 25 mM, where the micelle concentration would be one half that of the former solution. The fraction of bound micelles when *[DPS]* = 25 mM is less than that for *[DPS]* = 50 mM for any given fixed enzyme concentration. So the average *H* per micelle for [DPS] = 25 mM is greater than that for *[DPS]* = 50 mM. This rationalizes the observed differences in the degree of change in *H* between *[DPS]* = 25 mM and 50 mM with enzyme concentration. Such experiments with lipid mixed micelles are not possible because the enzyme would hydrolyze the lipids. Presence of binding even in the absence of lipid is treated as evidence of binding that is not lipid-specific and therefore variation in binding in the presence of lipid is neglected.

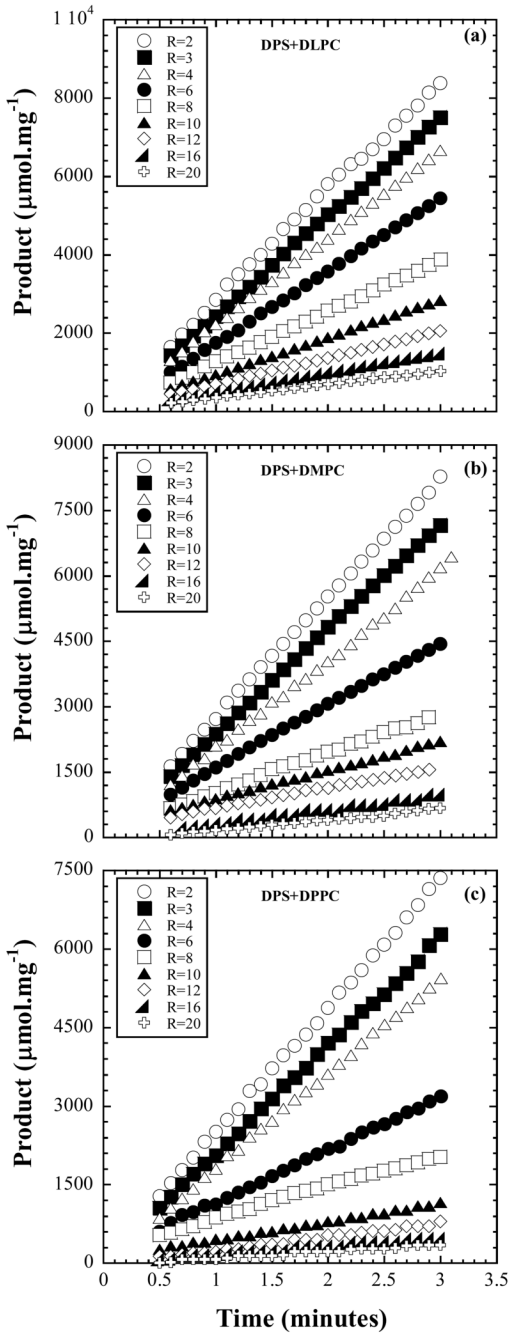

Figure 1.

Reaction progress curves of product formed due to activity of bacterial PLC on diacylphosphatidylcholine solubilized by DPS forming mixed micelles. Three different acyl lipid chain lengths were investigated. The data shown are for the surface dilution series obtained with [lipid] = 0.010 M and [DPS] = R[lipid]. The substrate concentration is diluted by increasing R.

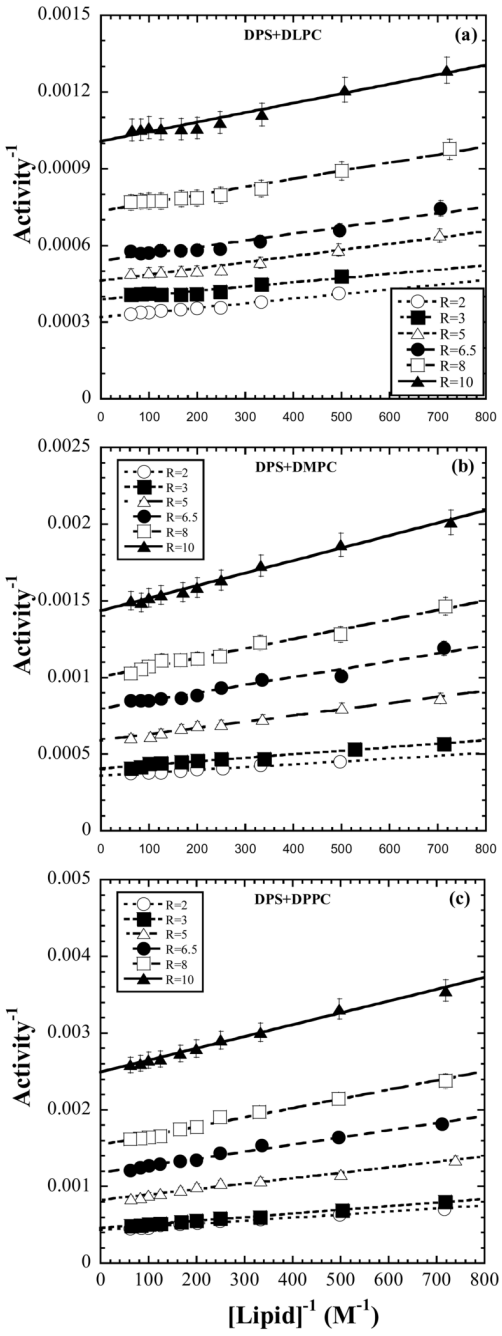

Figure 2.

Double reciprocal plots of inverse of the bacterial *PLC* micellar substrate activity vs. inverse of the molar concentration of phospholipid for six different micelle dilution series each of constant composition given by $R=\frac{[DPS]}{[lipid]}$ for each of the three lipids: (a) *DLPC*; (b) *DMPC*; (c) *DPPC* in mixed micelles with the surfactant *DPS*. The series is also described by constant *[S]* or constant X_{lipid}^{mic}. The solid lines are fits to the predicted linear variation of eq. 12.

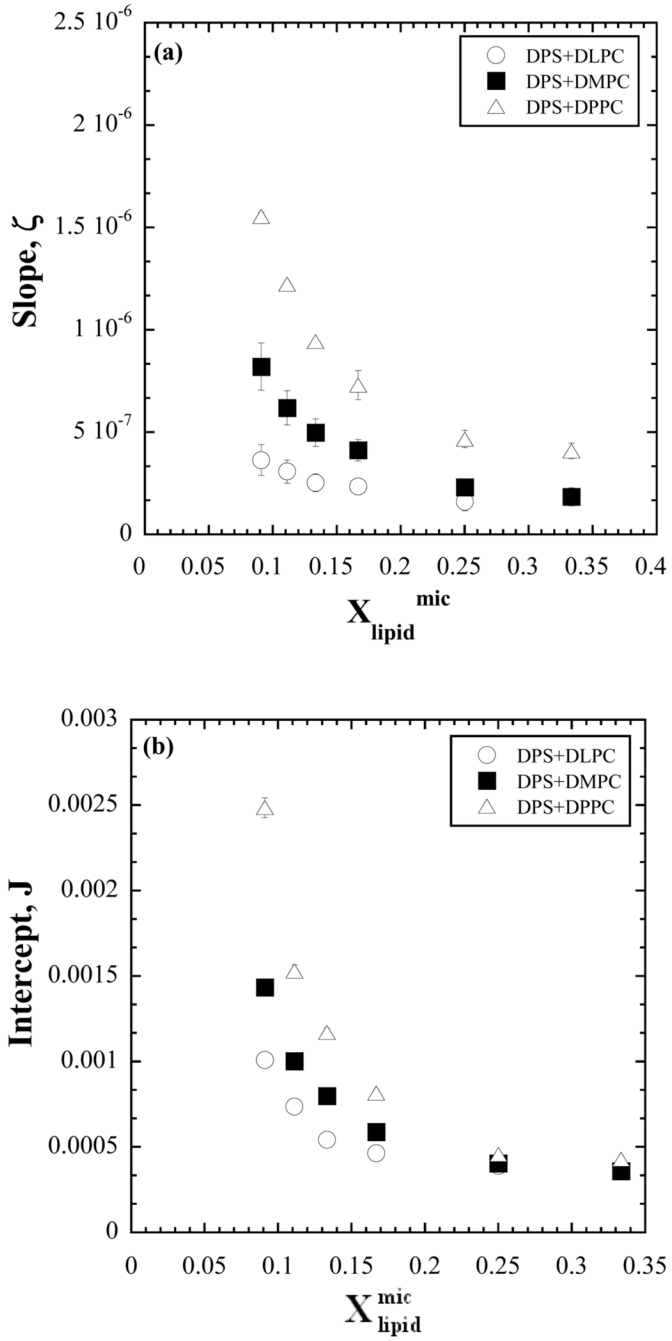

Figure 3.

Investigation of the variation with X_{lipid}^{mic} of the (a) slopes, ζ, and (b) intercepts, J, of the lines in Fig. 2. An exponential dependence is indicated.

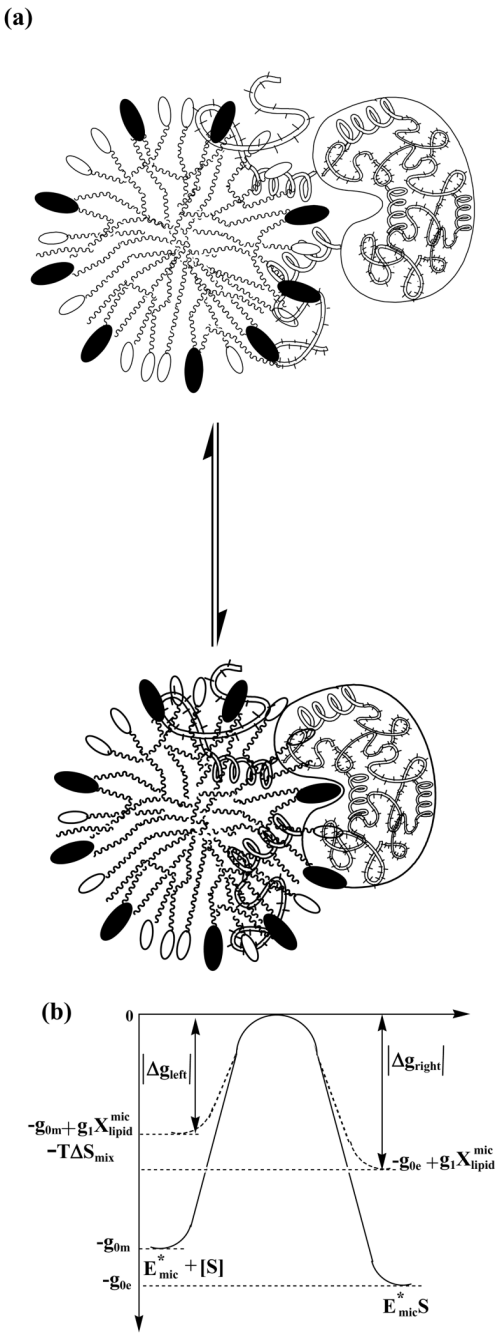

Figure 4.

(a) Visualization of the kinetic step (ii) for the binding between micelle solubilized lipid and micelle bound enzyme. (b) Proposed free energy model diagram showing the free energy levels of the two lipid states: micelle solubilized state (left) and enzyme bound state (right) and the free energy barrier.

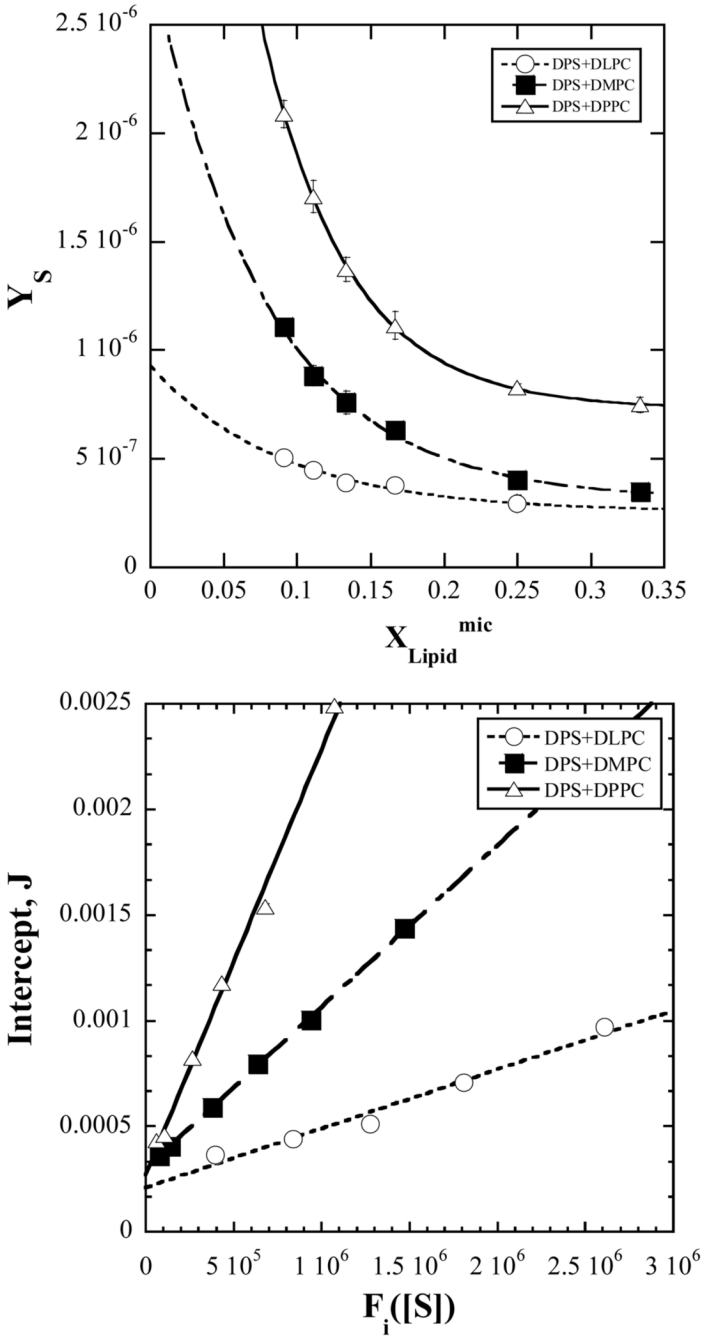

Figure 5.

(a) Observed micelle composition dependence of the modified slope, Y_S, and fits to the exponential variation predicted by the model in eq. 22. The fits yield g_1, $\frac{K_{M00}}{K_{M0}}$ and $\frac{K_{S0}K_{M0}a_0N_0}{k_3}$ for each of the investigated lipids.

(b). Data points are the observed intercepts J vs, the composition dependent function F_i *([S])* (defined by eq. 23). The line is that predicted by eq. 23 calculated with the values obtained in part (a) for the fit parameters g_1 and $\frac{K_{M00}}{K_{M0}}$.

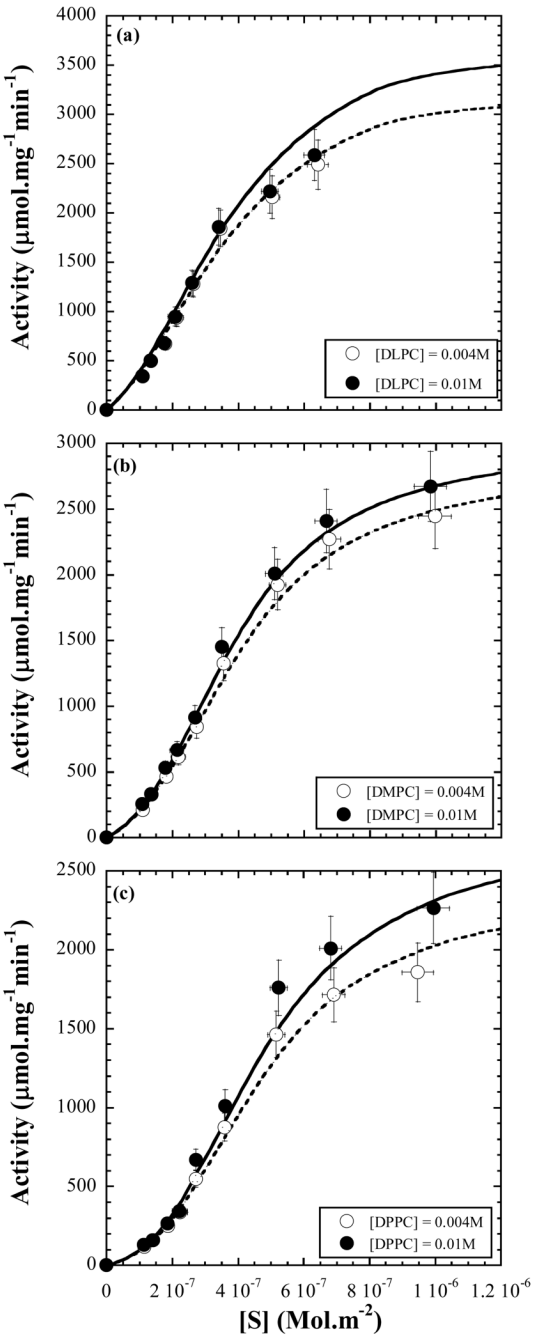

Figure 6.

The observed variation of the measured activity for the surface dilution series (constant *[lipid]* and varying *[DPS]*). The lines are the calculated variation according to eq. 10 and 11 with values of the kinetic constants and parameters predicted by fits of the data on the micelle dilution series to the interface kinetic model and the model for the kinetic parameters.

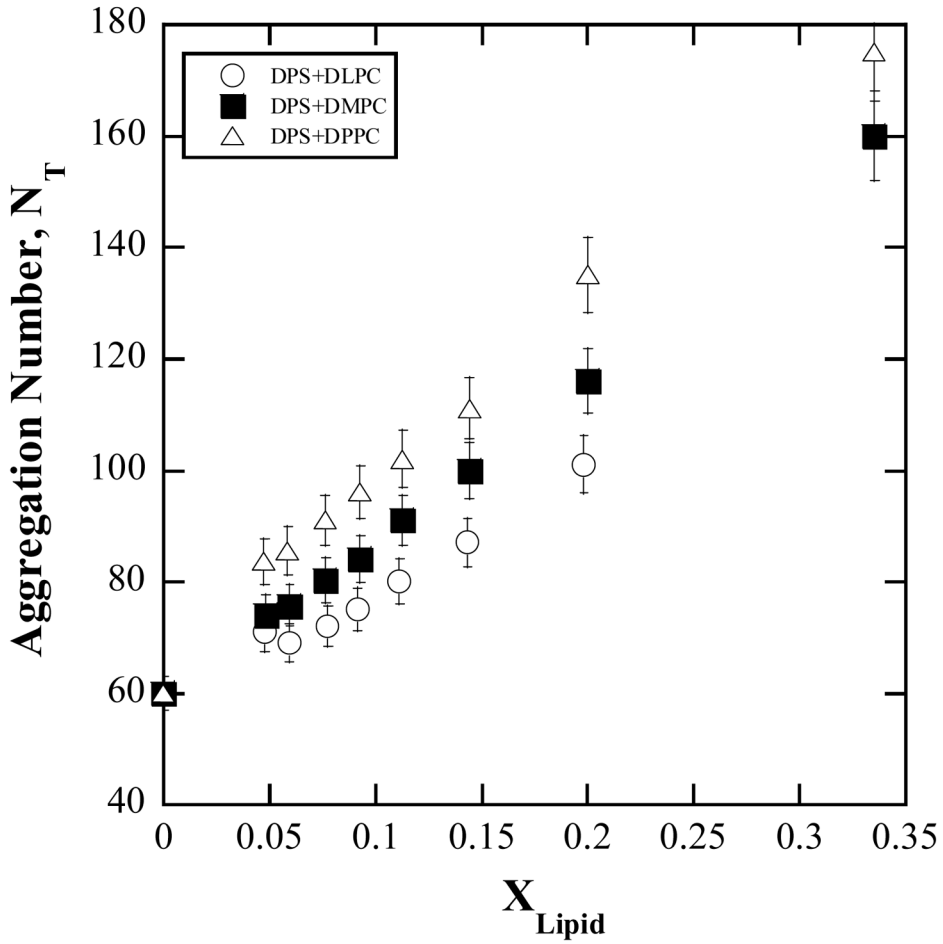

Figure A1.
Composition (molar fraction of lipid in solution) dependence of the total aggregation number, $N_T = N_{lipid} + N_{DPS}$ derived by *TRFQ* methods. Individual values of N_{lipid} and N_{DPS} can be easily determined from N_T and the composition [16].

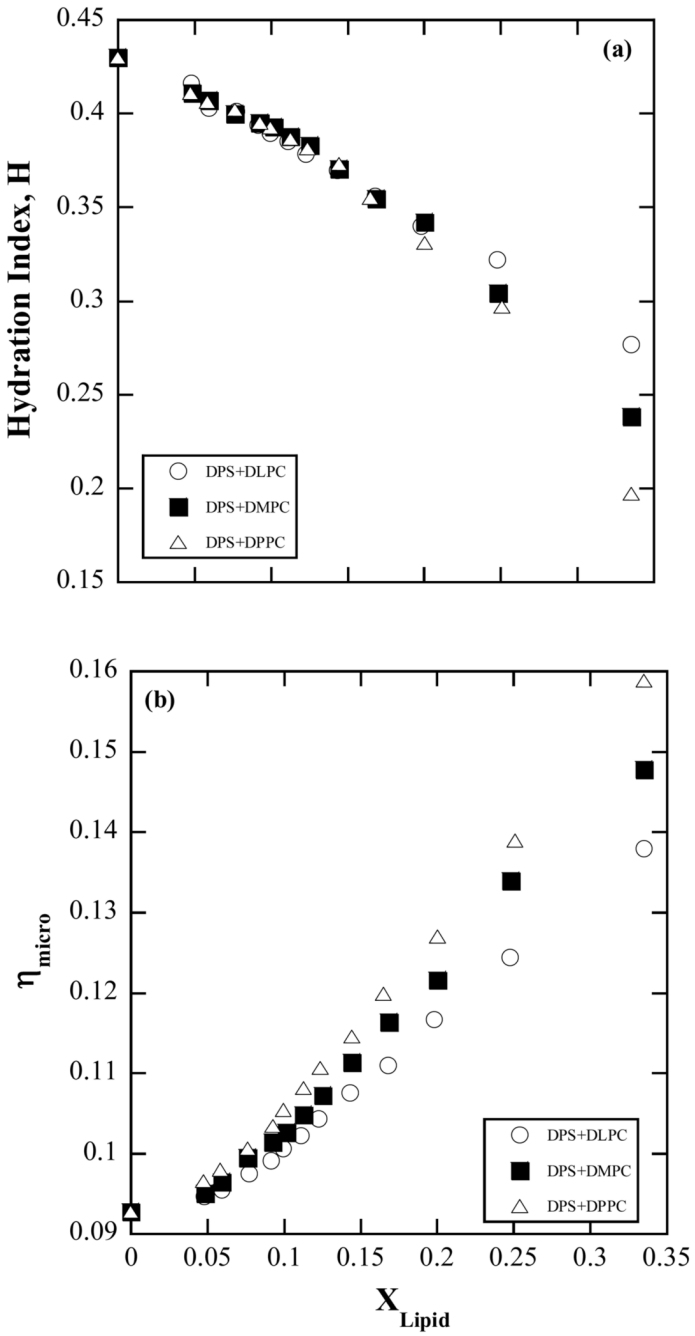

Figure A2.
Composition (molar fraction of lipid in solution) dependence of the (a) hydration index, *H*, and (b) interface microviscosity, $\eta_{micro,}$ obtained from *ESR* experiments.

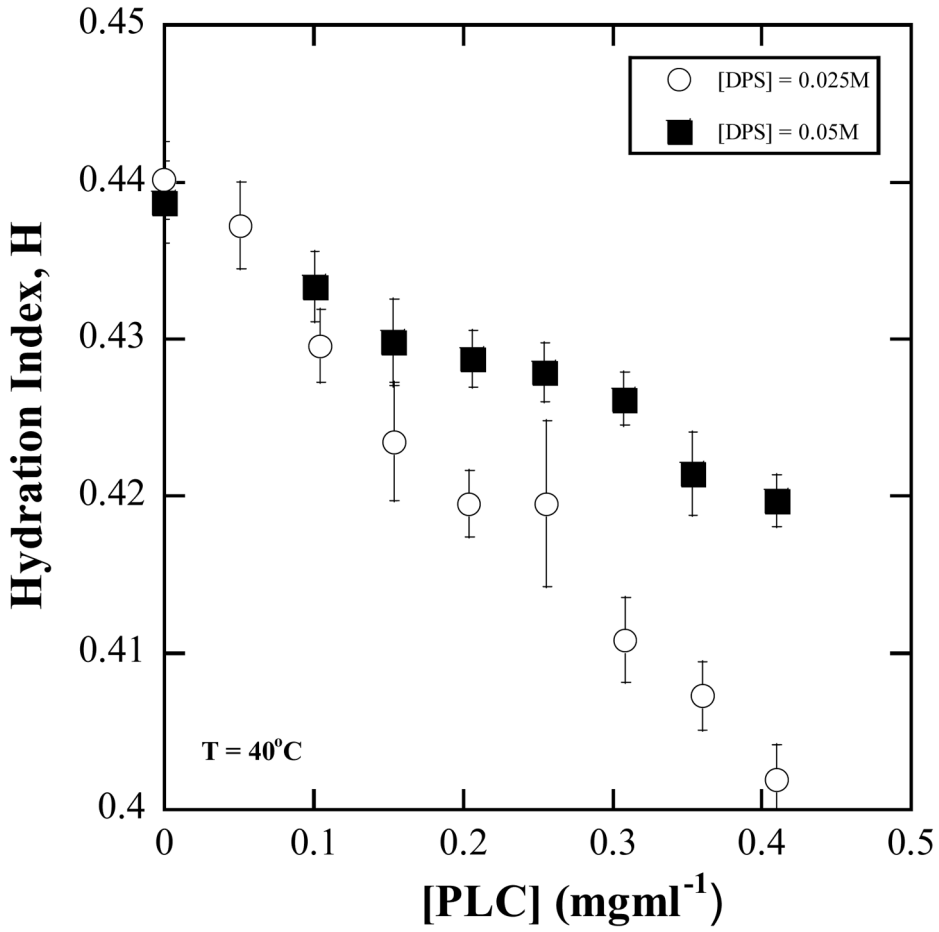

Figure A3.
Observations on *H* of *DPS* micelles at two different constant *[DPS]* concentrations of 25 mM and 50 mM. *H* decreases as enzyme is added to the micellar solution.

Table 1

Numerical values for the thermodynamic and kinetic parameters obtained from fits of the activity data to eq. 12 together with eq. 19 and 20.

phospholipid	$\frac{g_1}{RT}$ (a)	$K_{M0}/10^{-6}$ (Mm^{-2}) (b)	$K_{M00}/10^{-7}$ (Mm^{-2}) (c)	K_{S0} (mM) (d)	k_3 (μmol/min/mg)
DLPC	(11.3±5.4)	1.34±0.14	5.12±0.19	0.92±0.23	4797±964
DMPC	(12.8±1.6)	2.55±0.03	3.18±0.12	1.28±0.03	3333±80
DPPC	(17.1±0.6)	7.50±0.91	8.53±0.94	1.24±0.03	3723±590

(a) g_1 is the coefficient of the free energy of activation for lipid-enzyme binding as defined by eq. 17 and Fig. 4b.

(b) $K_{M0} = \frac{k_3}{k_{20}}$ (eq. 19 and 18)

(c) $K_{M00} = \frac{k_{-20}}{k_{20}}$ (eq. 19 and 18)

(d) $K_{S0} = \frac{k_{-1}}{k_1}$ (eq. 20)